Enhanced reflection from arrays of silicon based inverted nanocones

Haider Butt, Qing Dai, Ranjith Rajasekharan, Timothy D. Wilkinson, and Gehan A. J. Amaratunga[a),b)]
Electrical Engineering Division, Engineering Department, University of Cambridge, Cambridge CB3 0FA, United Kingdom

(Received 23 June 2011; accepted 12 August 2011; published online 27 September 2011)

We report enhanced reflection displayed by arrays of silicon based inverted nanocones. Theoretical studies suggest that such arrays display enhanced reflection and photonic band gaps within the optical and near infrared regions. Measured results show three to four fold enhancement in reflection and agree well with calculations. Such arrays can be used to enhance infrared reflection in photovoltaic devices which mostly contribute towards heating. © *2011 American Institute of*

Silicon nanopillars (NPs) are being explored in a number of applications. Their electrical properties have been used in solar cells,[1] photoluminescence and other photovoltaic (PV) devices.[2,3] Additionally, periodic arrays of cylindrical silicon (Si) nanopillars have also been shown to act as photonic crystals.[4] These NP lattice structures display band gap regions, with no allowed electromagnetic wave propagation, in the optical and infrared regions.

It has been reported that tapered and cone-shaped Si NPs produce refraction related optical losses in devices like two-dimensional (2D) planar photonic crystal waveguides.[5] Due to the index profile variation across the height of the nanocones (NCs), light propagating through their 2D lattice is refracted downward towards the cones bases which exhibit a higher refractive index.[6] This phenomenon has been used to produce Si NCs based antireflective coatings and to enhance the absorption in PV and other solar-energy harvesting applications.[7–9] Although there is a need to further improve absorption in the optical regime, at the same time it is also desirable to enhance the reflection in the infrared (IR) region which cannot be absorbed by the semiconductor. Such IR light which enters the PV cell leads to loss of performance through heating due to absorption on the back metal and substrate. This is a particularly severe problem for PV cells operating under concentrated light.

While following the same principle of increased absorption, the reflection of the desired frequencies from Si based surfaces can be enhanced by utilizing inverted cone shaped nanopillars. The refraction around the inverted cone suggests that the impinging radiation can be preferentially reflected back from the surface. We report in this paper the enhanced reflection displayed by square lattice periodic arrays of inverted silicon NCs. Arrays of inverted NCs having radius of the order 50 nm and the lattice constants of 300 nm and 400 nm are studied. Through theoretical studies, it was found that these high density arrays display photonic band gaps within the optical and near IR regime. Measured results were in excellent agreement with the calculations.

[a)]Electronic mail: gaja1@cam.ac.uk. Tel.: 44-1223-748320. FAX: 44-1223-748322.
[b)]Also with the Sri Lanka Institute of Nanotechnology, 14 Zone A EPZ, Biyagama, Sri Lanka.

The periodic arrays with nano-scaled dimensions, lattice constants a of the order 300–400 nm, display band gaps within the optical spectrum. To study the band gaps displayed by the square lattice arrays of Si NPs, theoretical analysis was conducted using the plane wave expansion (PWE) method. Square lattice arrays display band gap domains only towards light polarized parallel (transverse electric (TE)) to the NPs, while light polarized perpendicular (transverse magnetic (TM)) to the pillars propagates through the lattice. The calculated TE-mode band gaps displayed by the square lattice arrays with lattice constant $a = 300$ nm and 400 nm are shown in Figure 1. The dielectric constant for the NPs was set to $\varepsilon = 13 + 0.02i$.[4] The band diagrams show the normalized frequency plotted against the incident directions into the square lattice (G, X, and M as shown in Figure 1(c)). The TE-mode calculations show that the arrays with $a = 300$ nm displays three band gaps extending from 619 to 855 nm ($\omega a/2\pi c = 0.4838$-0.3401), 456 to 457 nm ($\omega a/2\pi c = 0.6542$ 0.6527), and 334 to 344 nm ($\omega a/2\pi c = 0.3338$-0.3438). The less dense array with $a = 400$ nm displays two band gaps extending from 805 to 970 nm ($\omega a/2\pi c = 0.497$-0.4115) and from 572.6 to 572.8 nm (0.6983-0.6981), as shown in Figures 1(a) and 1(b).

These photonic band gaps represent regions where no propagation through the lattice is allowed for incident light from every direction (G, X, and M). However, during the device characterization, the spectral measurements were performed for the incident light propagating in the X direction. Therefore, for the detailed analysis of the X direction band gaps and wave propagation through the arrays, finite element modeling (FEM) was performed. Figure 1(c) shows the simulated geometry used to calculate the light transmission through the lattice. For the purpose of simplicity, a 2D geometry of Si NPs of radius 50 nm and infinite heights was used, without considering the inverted cone shape. The cone shape leads to the superposition of different band gaps and changes their frequency ranges due to the interaction of light with varying radii of the cones. However, the localizations of the major band gaps remain the same.

The simulations were carried out for light ranging from 400 to 1600 nm and polarized both parallel (TE) and perpendicular (TM) to the axis of the silicon pillars. The calculated X direction transmission spectra through the arrays with

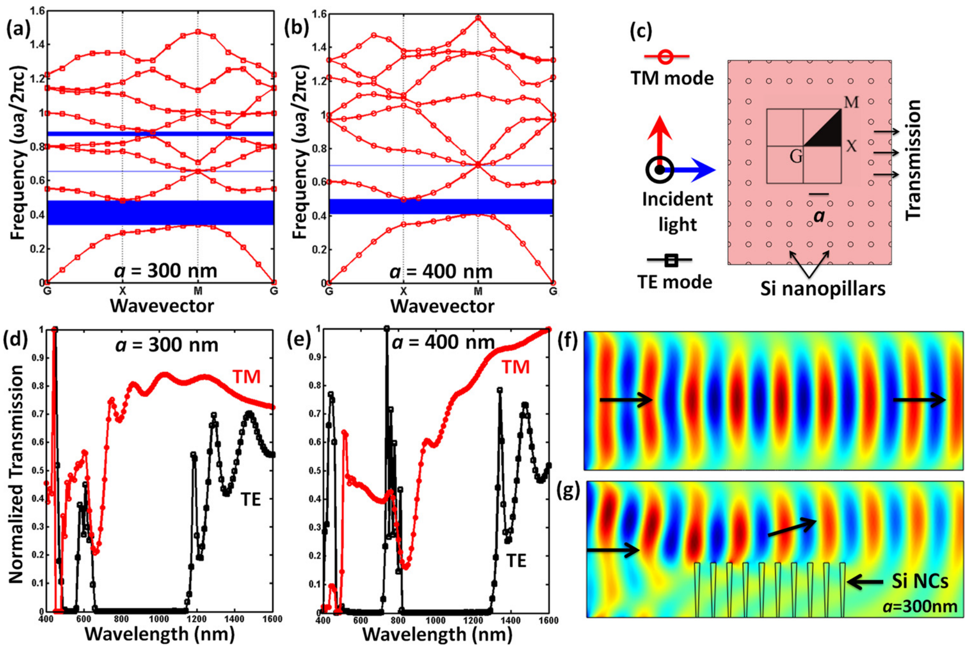

FIG. 1. (Color online) Calculated band gaps for square lattice arrays of Si NPs, with radius 50 nm and lattice constants (a) 300 nm and (b) 400 nm. (c) FEM model geometry used to simulate the X directed optical transmission spectrum through the lattice. Simulated transmission spectra for the NP arrays with a of (d) 300 nm and (e) 400 nm. (f) TM-mode wave propagation of an 800 nm wave through an empty cell. (g) Propagation of the same in the presence of Si NCs.

$a = 300$ nm and 400 nm are shown in Figures 1(d) and 1(e). The TE transmission spectrum for lattice with $a = 300$ nm show band gaps regions extending from 490 to 550 nm and 670 to 1150 nm. The arrays with $a = 400$ nm display band gaps from 470 to 710 nm and 820 to 1290. In both cases, the wider band gap of the two is associated with the Bragg condition $\lambda/2 \sim a$, where λ represents the wavelength in the photonic crystal. The localization of the two band gaps is consistent with the PWE simulation results, however, the frequency ranges are larger as they represent wave motion in only the X direction. Also no band gaps regions were observed in the TM transmission spectrum. Strong diffraction dips following the diffraction condition mentioned earlier are noticeable at 660 nm and 840 nm, for arrays with 300 nm and 400 nm lattice constants, respectively.

To study the effects of the inverted conical shape on the light propagation through the arrays, a 2D model was used and the propagation of an 800 nm wave through it simulated. The simulated wave propagation through the geometry with and without the array of inverted NCs (with $a = 300$ nm) is shown in Figures 1(f) and 1(g). A TM wave (with electric field parallel to the plane and axes of the NCs) propagates straight through the geometry when the NCs are not present. But in the presence of the inverted nanocones, the wave is refracted upwards demonstrating the enhanced reflection effect.

The fabrication of 2D arrays of Si inverted NCs was carried out using e-beam lithography to make the dot array pattern ($r = 50$ nm, $a = 300$ and 400 nm) on the Si substrate. The pattern was then sputtered with a metal mask (tungsten). The process of deep reactive etching was performed for etching the substrate. The array was then exposed to the following gases for a second each, in a succession lasting for 5 min: C_4F_8 for protective layering, O_2 for removing the C_4F_8 residues, and SF_6 for etching. The final etched substrate is shown in the scanning electron microscrograph (SEM) of Fig. 2. Well aligned and periodically patterned Si pillars are seen. The steepness of the cones was found to depend on the etching time.

The optical characterization of patterned arrays of Si NCs was carried out using an Ocean Optics white-light source having an optical spectrum from 450 nm to 1200 nm with a spectrometer. The polarization of the white-light beam was selected before the beam was guided onto the sample at an incidence angle of 80°. A series of microscope objectives were used to collimate and then focus the light beam onto the sample. To collect all the reflected light and to avoid any losses due to large angled diffraction orders, a high numerical aperture lens was placed very close to the sample. The reflected beam was focused into a feed fiber of an Ocean Optics 2000 spectrometer which had a spectral range extending from 500 nm to 1100 nm, with resolution 0.3 nm. The reflection spectrum measurements, as shown in Figure 3, are for the (X directed) unpolarized light and for light polarized parallel (TE) and perpendicular (TM) to the Si NCs. For each polarization of light, the reflection spectra were measured from the bare Si substrates and the arrays of inverted Si NCs. All the results were normalized with their respective reference reflection spectra measured from a front coated mirror.

The measured results, shown in Figure 3, are in good agreement with the simulations. The reflection spectra for the unpolarised light show the exact regions where the enhanced reflection effect was displayed by the NC arrays,

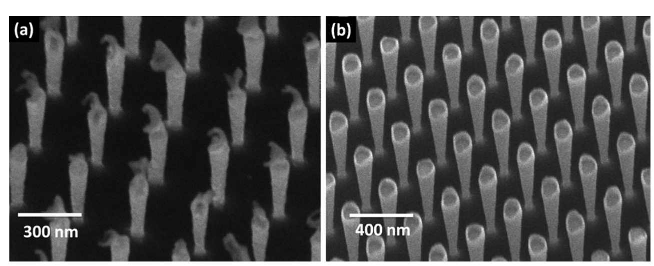

FIG. 2. SEM images of periodic arrays of inverted Si nanocones having radius of 50 nm and lattice constants (a) 300 nm and (b) 400 nm.

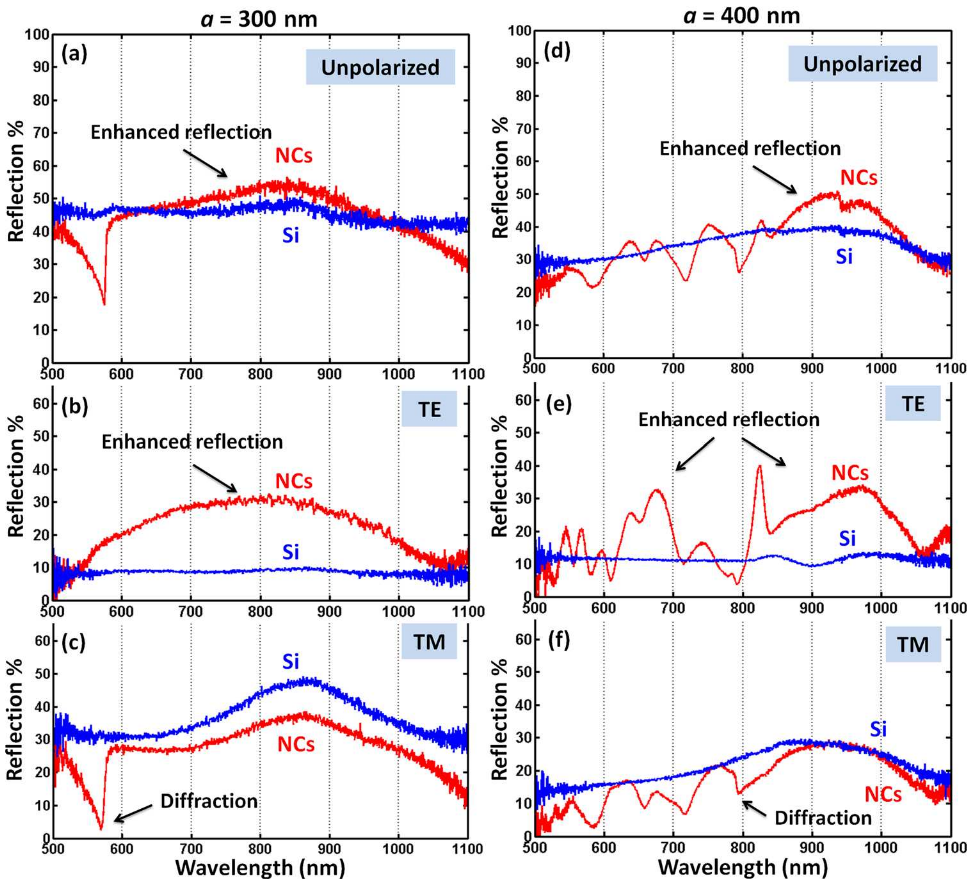

FIG. 3. (Color online) Measured reflection spectra from bare Si and Si based inverted NC array with spacing $a = 300$ nm, for (a) unpolarized (b) TE, and (c) TM mode of light. Reflection spectra from bare Si and inverted NC array with $a = 400$ nm, for (d) unpolarized (e) TE, and (f) TM mode of light.

with respect to bare Si. The NC arrays with $a = 300$ nm displayed enhanced reflection extending from 630 nm to 1000 nm. Whereas, the arrays with $a = 400$ nm displayed the major enhanced reflection regime extending from 850 nm to 1050 nm. The ranges show good agreement with the calculated band gaps and spectrum results.

The reflection measurements for the polarized light clearly demonstrate that the square lattice NC arrays display band gaps and consequently the enhanced reflection only for the TE polarization of light. The arrays with 300 nm spacing display an enhanced TE-mode reflection of the order 3 times higher than Si, encompassing almost the entire optical regime and both the band gaps predicted by the calculations. The overlapping of band gaps is due to the different radii of the cone interacting with the incident light.[6] The arrays with 400 nm spacing displayed a succession of enhanced TE reflection bands, with major ones extending from 620 nm to 710 nm and from 805 nm to 1100 nm and beyond. Due the spectral limitation of the light source and spectrometer used, exact upper wavelength limits of the second band could not be measured. The maximum enhanced reflection effect displayed by the 400 nm array was of the order 4 times higher relative to bare Si in the IR region extending from 805 nm onwards. This is of interest, here, as this paves way towards utilization of such structures for enhancing IR reflection in solar cells and other photovoltaic applications. The TM-mode reflections results displayed no enhanced reflection effect. Most important features in the TM reflection spectra were the strong diffraction dips observed near 575 nm and 795 nm for the arrays with lattice constants 300 nm and 400 nm, respectively.

In conclusion, we have demonstrated three to four fold enhanced reflection, relative to bare Si substrates, by utilizing the periodic arrays of inverted silicon nanocones. By utilizing square lattice arrays which display band gaps only for the TE light, we confirm that these inverted nanocone arrays display enhanced reflection strictly in their photonic band gaps. The enhanced reflection regions can be tailored in the desired frequency regimes by engineering and optimizing the array geometries. Arrays with 400 nm lattice constants have shown enhanced reflection in the IR regime which paves the way towards their utilization in PV devices to increase IR reflection and minimize heating.

This work was partly funded under the Nokia-Cambridge Strategic Partnership in Nanoscience and Nanotechnology (Energy Programme). The authors also thank Jeremy Baumberg and Petros Farah for fruitful discussions. H.B. and Q.D. contributed equally to this work.

[1] E. Garnett and P. Yang, Nano Lett. **10**, 1082 (2010).
[2] G. Burak, M. Evren, W. Xiaodong, P. Kin Leong, and D. Hilmi Volkan, Appl. Phys. Lett. **97**, 093111 (2010).
[3] Z. Hang, C. Alan, A. Arman, Y. Yang, R. Nalin, B. Tim, H. Ibraheem, H. Pritesh, N. Arokia, and A. J. A. Gehan, Adv. Mater. **21**, 3919 (2009).
[4] V. V. Poborchii, T. Tada, and T. Kanayama, J. Appl. Phys. **91**, 3299 (2002).
[5] Y. Tanaka, T. Asano, Y. Akahane, B.-S. Song, and S. Noda, Appl. Phys. Lett. **82**, 1661 (2003).
[6] G. W. Burr, S. Diziain, and M. P. Bernal, Opt. Express **16**, 6302 (2008).
[7] J. Zhu, Z. Yu, G. F. Burkhard, C.-M. Hsu, S. T. Connor, Y. Xu, Q. Wang, M. McGehee, S. Fan, and Y. Cui, Nano Lett. **9**, 279 (2008).
[8] Y. Hung, Jr., S.-L. Lee, and L. A. Coldren, Opt. Express **18**, 6841 (2010).
[9] M. D. Kelzenberg, S. W. Boettcher, J. A. Petykiewicz, D. B. Turner-Evans, M. C. Putnam, E. L. Warren, J. M. Spurgeon, R. M. Briggs, N. S. Lewis, and H. A. Atwater, Nat. Mater. **9**, 239 (2010).